Journal of the Korean Society of Marine Engineering, Vol.30, No.4, pp.483~493, 2006(ISSN 1226-9549)

Modeling of Pressure Drop for Water Vapor Flow across Tube Banks inside Horizontal Tube Absorber

Thanh Tong Phan* · Jung-In Yoon† · Eun-Pil Kim**

(Manuscript : Received MAY 15, 2006 ; Revised MAY 29, 2006)

Abstract : A model for a pressure drop of water vapor flow across tube banks in a horizontal tube absorber of an absorption chiller/heater using LiBr solution as a working fluid has been developed based on a commercial 20RT(70kW) absorption chiller/heater. The numerical results show that the characteristic of the pressure drop in the shell side of the horizontal tube absorber is completely different from that in a conventional shell and tube heat exchanger. Especially, solution film thickness has significant influence on the vapor pressure drop in the horizontal tube absorber. In addition, the effects by the tube diameters, the longitudinal pitch to diameter ratio, and Reynolds number of the vapor flow, on the vapor pressure drop have been studied to evaluate the compactness of tube absorber. It was found that the vapor pressure drop decreases as tube diameter increases, the longitudinal pitch to diameter ratio increases, and Reynolds number of the vapor flow decreases. A comparison of the present study results with well-established experimental and numerical results showed a good overall agreement.

Key words : Tube absorber, Absorption chiller/heater, Pressure drop, Solution film thickness

Nomenclature

C_f : skin friction coefficient
d : tube diameter, m
p : pressure, Pa
S_L : longitudinal pitch, m
S_T : transverse pitch, m
u : streamwise velocity, m/s
v : crosswise velocity, m/s
x : streamwise displacement, m
y : crosswise displacement, m

Greek letters

α : under-relaxation factor
δ : solution film thickness, m
μ : dynamic viscosity, kg/ms
ρ : density, kg/m^3
τ : shear stress, N/m^2
Φ : general dependent variable

† Corresponding Author(School of Mechanical Engineering, Pukyong National University, KOREA). E-mail: yoonji@pknu.ac.kr, Tel: 051)620-1506
* Graduate School, Department of Refrigeration and Air-conditioning Engineering, Pukyong National University, KOREA.
** School of Mechanical Engineering, Pukyong National University, KOREA.

Γ : solution mass flow rate per unit length, kg/ms

Subscripts

s : solution film
v : vapor
w : tube wall
∞ : free stream

1. Introduction

Absorption refrigeration is an alternative approach for cooling, which is thermally driven and requires a little external work. This type of refrigeration is getting more important for reducing the thermal pollution to environment. Absorption systems can be used with an inexpensive thermal energy source such as solar energy and waste heat. However, the size of absorption chiller/heater is larger than that of the vapor compression type chiller/heater based on the same capacity. Among these components, the absorber, which effects directly on efficiency, size, manufacturing and operating cost of the system, is least understood[1]. In the horizontal tube absorber, the pressure drop of water vapor at the shell side influences to the internal working pressure of the absorber, and hence effects on the absorption capacity of the absorber. The size of absorber can be reduced by replacing the conventional diameter heat exchanger tubes with the smaller diameter heat exchanger tubes. Most of previous studies were carried out on the fluid flow with the crossflow type in the tube banks of a conventional shell and tube heat exchanger. Nishimura[2] studied detailed results from a finite element method analysis for equal spacing arrangement of the tube banks with pitch to diameter ratios of 1.33, 1.6, and 2.0 at Reynolds numbers between 1 and 40. Zdravistch et al.[3] used the finite volume method and reported results for an equal spacing arrangement with pitch to diameter ratios of 2.0 at Reynolds numbers equal to 54. Wang et al.[4] presented results for fluid flow at nominal pitch to diameter ratios of 1.25, 1.5 and 2.0 for equilateral triangle and rotated squared tube arrangements with Reynolds numbers of 100 and 300. Wilson et al.[5] predicted pressure drop and heat transfer in laminar and turbulent flow of air across tube banks. However, the study on the pressure drop of tube banks inside absorber has been lacked. Suzuki et al.[6] developed a model of two-dimensional of vapor flow in the absorber/evaporator of the absorption chiller and reported the effect of pitch to diameter ratio to vapor pressure drop and absorption mass flux.

In this study, a model of the pressure drop for a water vapor flow across tube banks inside horizontal tube absorber of absorption chiller/heater using LiBr solution as a working fluid has been developed based on a commercial 20RT (70kW) absorption chiller/heater. The characteristic of the pressure drop in the shell side of the horizontal tube absorber, especially the effect of solution film thickness on the pressure drop of the absorber was investigated by comparing with the pressure drop of a conventional shell and tube heat exchanger. In addition, the effect of tube diameters

which were changed from 15.88mm to 12.7mm and 9.52mm, longitudinal pitch to diameter ratio S_L/d, and vapor Reynolds number on the vapor pressure drop, have been studied to evaluate the compactness of the tube absorber.

Table 1 Specification of absorber of 20RT(70kW) commercial absorption chiller/heater

Parameters	Values
Tube length [m]	2
Diameter [m]	0.01588
Number of columns of tube bank	13
Number of rows of tube bank	35
Number of tubes in tube bank	228
Longitudinal pitch [m]	0.017
Transverse pitch [m]	0.02562
Longitudinal pitch to diameter ratio	1.07
Width of absorber [m]	0.238
Height of absorber [m]	0.46118
Volume of absorber [m^3]	0.2195
Cooling capacity of evaporator [RT]	20
Total vapor mass flow rate [kg/s]	0.0283
Vapor temperature [°C]	5
Vapor Reynolds number	56
Inlet solution temperature [°C]	47
Inlet solution concentration [wt%]	61
Solution film Reynolds number	30
Physical properties of saturated water vapor	
Density [kg/m^3]	0.0068
Dynamic viscosity [kg/ms]	9.34×10^{-6}
Heat of evaporation [kJ/kg]	2488.69
Physical properties of LiBr solution	
Density [kg/m^3]	1732.838
Dynamic viscosity [kg/ms]	0.004933

2. Analysis model of pressure drop for water vapor flow

2.1 Analysis model and assumptions

In the absorber, the LiBr solution film composed of LiBr (absorbent) liquid and water (refrigerant) flows down over tube surfaces. The film solution is in contact with the water vapor which comes from an evaporator. As the water vapor pressure is higher than the partial pressure of liquid water in solution, the water vapor is absorbed into solution. The amount of the absorbed vapor depends on the water vapor pressure. The pressure drop is developed as the vapor flow across the tube banks and influences to the water vapor pressure and therefore, effects on the amount of absorbed vapor. The pressure drop of a tube absorber is different from that of a conventional shell and tube heat exchanger in calculation since there is absorption process occurred inside the absorber. It causes water vapor to be completely absorbed into LiBr solution, which results in no flow at the outlet absorber. Also, during falling down outside tube surface, the droplets and falling films of solution prevent the flow motion therefore it causes increasing of vapor pressure drop.

Table 1 shows the specifications of absorber of 20RT commercial absorption chiller/heater. The photo of tube banks in evaporator and absorber is shown in fig. 1. Based on this reference absorber, a model of pressure drop for water vapor flow across the tube banks inside absorber was performed as shown in fig. 2. The tube banks are uniform and staggered, the water vapor flows across tube banks in x direction. Due to symmetry of the tube banks and the periodicity of the flow inherent in the tube banks geometry as shown in fig. 2, only a portion of the geometry is modeled, with symmetry applied to the outer boundary. The inflow boundary is redefined as a periodic zone,

and the outflow boundary defined as its shadow.

In formulating this model, the following assumptions have been made:

- The vapor flow is incompressible, steady and laminar.
- Neglecting effect of solution droplets on pressure drop, only the effect of solution falling films have been calculated.
- The flow of solution film is assumed to be laminar in which the film surface is smooth and its thickness is constant. Fig. 3 shows the calculation domain of tube banks model inside horizontal tube absorber showing solution film thickness which is determined by Nusselt's analysis[7] as follows:

$$\delta = \left(\frac{3 \Gamma_s \mu_s}{\rho_s^2 g} \right)^{1/3} \tag{1}$$

And solution film Reynolds number is defined as follows:

$$Re_s = \frac{4 \Gamma_s}{\mu_s} \tag{2}$$

- Because there is no vapor flow at the outlet absorber, therefore the mass flow rate of absorbed vapor is assumed reduced 50%.

2.2 Governing equations and boundary conditions

For 2-dimensional laminar flow with constant fluid and material properties, also negligible buoyancy, the governing equations for mass and momentum in a steady state flow are given by:

Continuity:

$$\frac{\partial u_v}{\partial x} + \frac{\partial v_v}{\partial y} = 0 \tag{3}$$

x-momentum:

$$\rho_v \left(u_v \frac{\partial u_v}{\partial x} + v_v \frac{\partial u_v}{\partial y} \right) = -\frac{\partial p_v}{\partial x} + \mu_v \left(\frac{\partial^2 u_v}{\partial x^2} + \frac{\partial^2 u_v}{\partial y^2} \right) \tag{4a}$$

y-momentum:

$$\rho_v \left(u_v \frac{\partial v_v}{\partial x} + v_v \frac{\partial v_v}{\partial y} \right) = -\frac{\partial p_v}{\partial y} + \mu_v \left(\frac{\partial^2 v_v}{\partial x^2} + \frac{\partial^2 v_v}{\partial y^2} \right) \tag{4b}$$

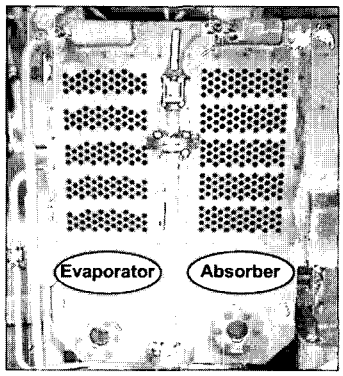

Fig. 1 Photo of tube banks in absorber of 20RT(70kW) commercial absorption chiller/heater

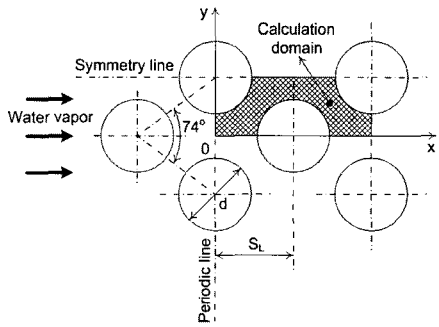

Fig. 2 Schematic of tube banks model inside horizontal tube absorber

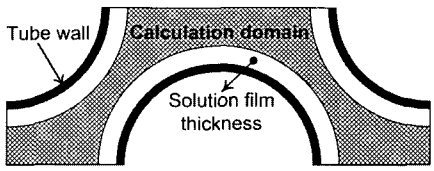

Fig. 3 Calculation domain of tube banks model inside absorber showing solution film thickness (not to scale, film thickness greatly exaggerated)

At the tube wall, no slip boundary condition ($u_v = v_v = 0$) are imposed on the tube surfaces. The material of tube is assumed to be copper.

The symmetry boundary conditions shown in fig. 1 satisfy the conditions:

$$\frac{\partial u_v}{\partial y} = 0 \quad v_v = 0 \tag{5}$$

The concepts of periodic boundary condition shown in fig. 2 have been described by Patankar et al.[8].

2.3 Method of numerical analysis

A CFD software, Fluent[9], is used for the numerical analysis. The studied model shown in fig. 4 is created and meshed by using Gambit software. Quadrilateral cells that provide better resolution of the viscous gradients near the tube wall are used in the regions surrounding the tube walls whereas triangular cells are used for the rest of domain, resulting in a hybrid mesh with 5792 cells. Then, the created model in Gambit software is exported to the Fluent software in which boundary conditions and material properties are defined. The governing equations along with the boundary conditions were solved for the velocity components, u and v, the pressure p. A segregated solution approach using the SIMPLEC algorithm, as implemented in Fluent[9], is used to link the pressure and velocity fields. The algorithm is described in the Ref. [10].

Convergence to steady state was monitored using calculation of the change of variable Φ. This is typical achieved by under-relaxation, which reduces the change of Φ produced during each iteration. In a simple form, the new value of the variable Φ within a cell depends upon the old value, Φ_{old}, the computed changed in Φ, $\Delta\Phi$, and the under-relaxation factor, α, as follows:

$$\Phi = \Phi_{old} + \alpha\Delta\Phi \tag{6}$$

where variable Φ, general dependent variable, is u, v, p. The value of α was checked at all nodal locations and convergence was declared when the maximum values of α were typically less than 1×10^{-5}.

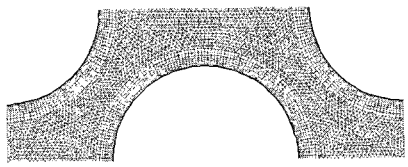

Fig. 4 Grid system of calculation domain

3. Numerical results and discussions

The numerical conditions of this study are based on a normal operating condition of absorber of 20RT commercial absorption chiller/heater shown in table 1. A variable parameter such as the tube diameter, the longitudinal pitch, the longitudinal pitch to diameter ratio S_L/d, vapor and solution Reynolds number is varied to investigate its effect on vapor pressure drop whereas another are fixed at the normal operating condition. The computing program is run for each different input data case to obtain the numerical results. The typical velocity distribution of vapor flow at the normal operating condition of absorber is shown in fig. 5. The typical pressure distribution is shown in fig. 6, as well. As mentioned earlier about periodic boundary condition, the

resulting velocity and pressure fields show completely periodic.

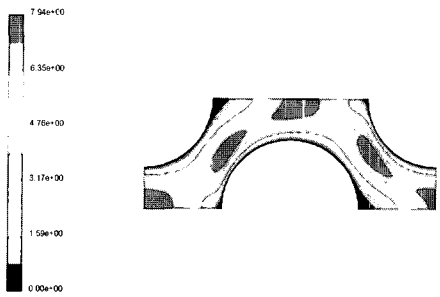

Fig. 5 Velocity distribution of vapor flow

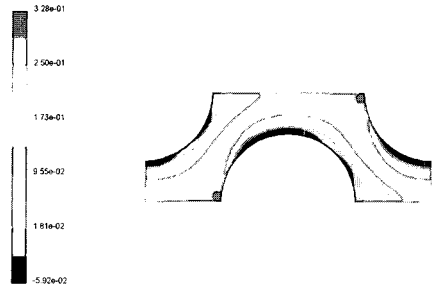

Fig. 6 Pressure distribution of vapor flow

3.1 Comparison with previous works

In order to test the validation of the solution procedure, it is essential that CFD simulations must be compared with experimental data. Comparison with previous numerical and experimental studies shows in fig. 7 and 8. The comparison is base on a dimensionless parameter used to represent the hydraulic resistance, which is so-called the skin friction coefficient C_f

$$C_f = \frac{\tau_w}{\frac{\rho_v u_{v,\infty}^2}{2}} \qquad (7)$$

where τ_w is the wall shear stress on the tube surface at an angle Θ from the front of tube and $u_{v,\infty}$ is the free streamwise velocity of vapor at the inlet.

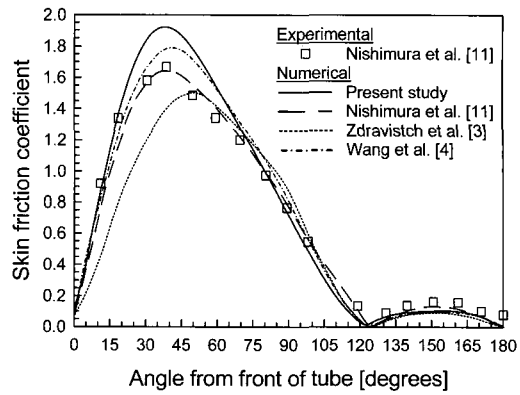

Fig. 7 Distribution of skin friction coefficient at $Re_{v,\infty}$ = 54 with $S_L/d = S_T/d = 2$

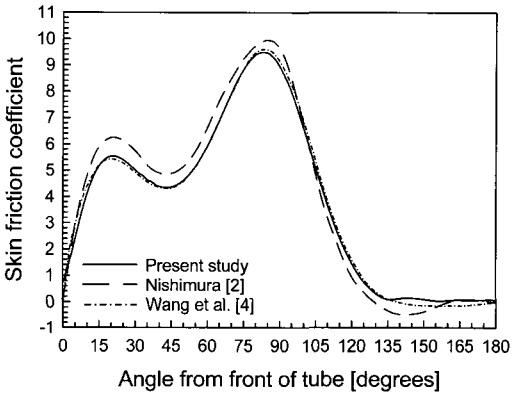

Fig. 8 Distribution of skin friction coefficient at $Re_{v,\infty}$ = 20 with $S_L/d = S_T/d = 1.33$

Fig. 7 shows the variation of the skin friction coefficient with the angle from the front of tube at $S_L/d = S_T/d = 2$ and $Re_{v,\infty} = 54$. The experimental and numerical results of Nishimura et al.[11] are plotted with the numerical results of Zdravistch et al.[3], Wang et al.[4] and the present results. This is good agreement between the present results and the experimental results of Nishimura et al.[11]. While the prediction of Nishimura et al.[11] and Wang et al.[4] are closer to the experimental data, the present results are within the experimental uncertainly, which was reported to be 10 - 15%.

Fig. 8 is plots of the results of the present work and the numerical results of Nishimura[2] and Wang et al.[4] for local skin friction coefficient around a typical tube within the bank with $S_L/d = S_T/d = 1.33$ and $Re_{v,\infty} = 20$. The trends of the results agree well. The magnitudes of the results obtained by the present study and Wang et al.[4] agree well but show little different from those of Nishimura[2].

As shown in fig. 7 with fig. 8, it can be found that the numerical results of this study agree well with study of Wang et al.[4] whereas little different from another studies since this study and the study of Wang et al.[4] used the same maximum value of under-relaxation factor α for u, v and p which is typically less than 1×10^{-5}.

3.2 Comparison of pressure drop between heat exchanger and absorber

Fig. 9 shows the comparison of the effect of the ratio S_L/d on the pressure drop between conventional shell and tube heat exchanger and horizontal tube absorber. The comparison condition is vapor Reynolds number is the same at $Re_{v,\infty} = 56$. In the case absent solution falling films on the tube surfaces, solution film thickness is $\delta = 0$, the pressure drop of absorber is smaller than pressure drop of heat exchanger. It can be explained that during vapor flows across the tube banks inside absorber, the vapor is absorbed into solution hence the vapor mass flow rate is reduced resulting in vapor pressure drop is decreased.

However, in actually, there are solution falling films on tube surfaces make the pressure drop of absorber increases. As shown in the figure, at the normal operating condition of absorber, solution film Reynolds number is $Re_s = 30$ then solution film thickness $\delta = 0.266$mm, the pressure drop of absorber is higher than pressure drop of heat exchanger at the low value of ratio S_L/d.

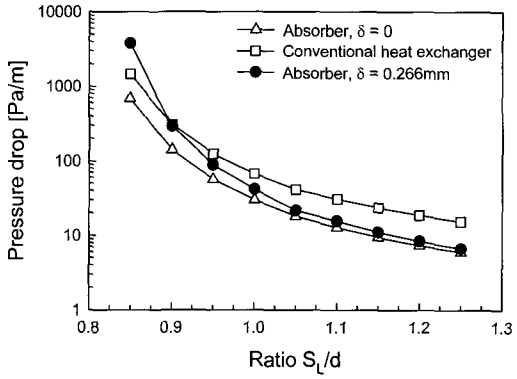

Fig. 9 Comparison of effect of ratio S_L/d on pressure drop between heat exchanger and absorber

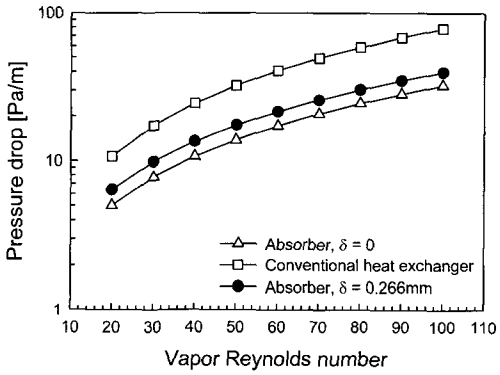

Fig. 10 Comparison of effect of vapor Reynolds number on pressure drop between heat exchanger and absorber

The comparison of the effect of vapor Reynolds number on the pressure drop between conventional heat exchanger and horizontal tube absorber is shown in fig. 10 with the same ratio $S_L/d = 1.07$ and at the normal operating condition of absorber. When vapor Reynolds number increases, the vapor velocity increases, it causes the

vapor pressure drop increases. As shown in the figure, the pressure drop of absorber is smaller than pressure drop of heat exchanger. It can be explained that although the vapor pressure drop increases with the present of solution films on the tube surfaces, but the value of solution film thickness at the normal operating condition is not high enough to causes the vapor pressure drop of the absorber increases over the value of pressure drop of the heat exchanger.

3.3 Effect of solution film thickness

Fig. 11 shows the effect of solution film thickness with variation of the ratio S_L/d at the normal operating condition vapor Reynolds number $Re_{v,\infty}$ = 56. As solution film thickness increases, it strongly prevents the motion of the vapor flow therefore the vapor pressure drop increases. Especially, at the low ratio S_L/d, S_L/d = 0.85, the spacing of tubes in the bank is very narrow therefore the increase of solution film thickness effects significantly to the pressure drop.

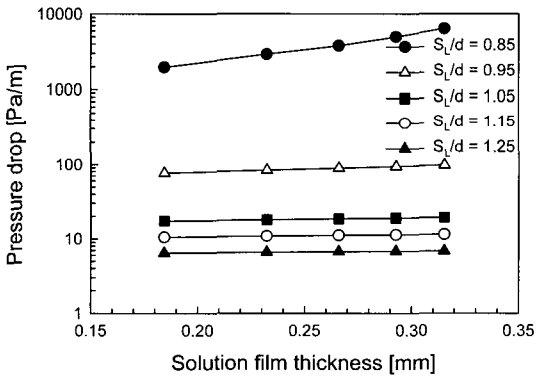

Fig. 11 Effect of solution film thickness with variation of ratio S_L/d

The effect of solution film thickness on pressure drop with variation of vapor Reynolds number at the ratio S_L/d = 1.07 is shown in fig. 12. The effect of solution film thickness on pressure drop is steady as vapor Reynolds number varying.

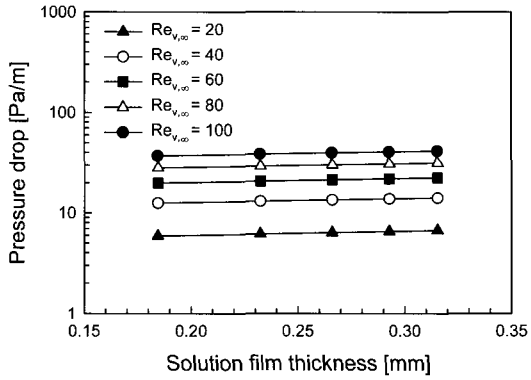

Fig. 12 Effect of solution film thickness with variation of vapor Reynolds number

3.4 Effect of tube diameter

In order to compare the effect of three different tube diameters 15.88mm, 12.70mm and 9.52mm on vapor pressure drop, the volume of absorber is kept at constant as shown in table 1, V = 0.2195m3, whereas vapor Reynolds number and the ratio SL/d are varied. The effects of these parameters on pressure drop are investigated with the present of solution film thickness on the tube surfaces since the solution film thickness really plays an important roll on the pressure drop of absorber at the shell side as mentioned above. The solution film thickness is chosen at δ = 0.266mm according to the normal operating condition.

Fig. 13 presents the effect of longitudinal pitch to diameter ratio S_L/d on pressure drop per unit length of the tube banks in flow direction with vapor Reynolds number is kept at the normal operating condition

$Re_{v,\infty}$ = 56. In designing absorber, it is necessary to decrease the ratio S_L/d in order to decrease the absorber size. However as shown in the figure, it makes the pressure drop increases, resulting in working pressure inside absorber increases. That means it exists an optimal longitudinal pitch to diameter ratio S_L/d which is minimizes the tube absorber volume, it is about 1.0 to 1.1 depending on the tube diameter.

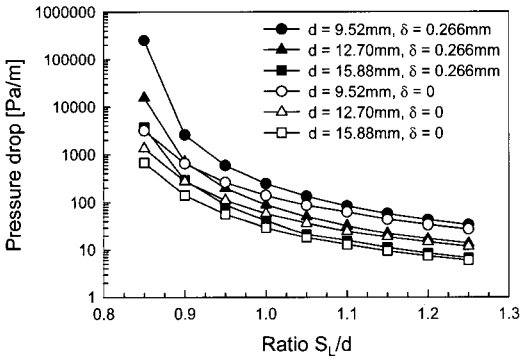

Fig. 13 Effect of ratio S_L/d on pressure drop

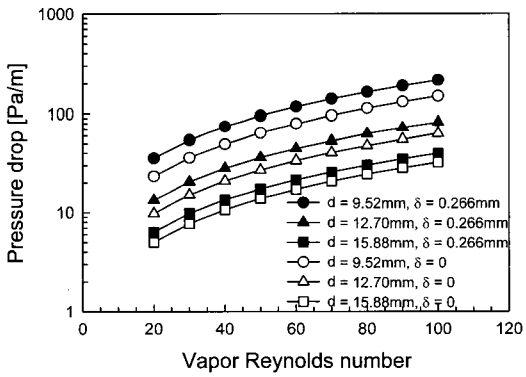

Fig. 14 Effect of vapor Reynolds number on pressure drop

About the effect of tube diameter, as shown in this figure, pressure drop of small diameter tube is higher than the pressure drop of larger diameter tube at the same longitudinal pitch to diameter ratio S_L/d.

Fig. 14 shows the effect of vapor Reynolds number on pressure drop per unit length of the tube banks in flow direction with the longitudinal pitch to diameter ratio S_L/d = 1.07. The pressure drop increases as vapor Reynolds number increases.

The trend of vapor pressure drop variation as tube diameter decreases is similar in fig. 13 and 14. Therefore, it is clear that the vapor pressure drop decreases as tube diameter increases at the same vapor Reynolds number and longitudinal pitch to diameter ratio S_L/d.

The variation of vapor pressure drop in the case of absent solution falling films on the tube surfaces is also expressed in fig. 13 and 14 to evaluate the effect of solution film thickness on vapor pressure drop. This matter has been discussed in fig. 11 and 12.

4. Conclusions

A model of pressure drop for water vapor flow across tube banks inside horizontal tube absorber has been developed. The results can be summarized as follows:

The characteristic of pressure drop in the shell side of the horizontal tube absorber is completely different from that in a conventional shell and tube heat exchange. In the case absent solution falling films on the tube surfaces the pressure drop of absorber is smaller than the pressure drop of heat exchanger.

In actually, there are solution falling films on tube surfaces. The vapor pressure drop in horizontal tube absorber is

influenced significantly by solution film thickness. The vapor pressure drop increases as solution film thickness increases. Especially the pressure drop of absorber is higher than pressure drop of heat exchanger at the low value of longitudinal to diameter ratio S_L/d.

The vapor pressure drop decreases as tube diameter increases, longitudinal pitch to diameter ratio increases and vapor Reynolds number decreases. Among three different tube diameters, the smallest tube diameter 9.52mm has highest vapor pressure drop.

It is confirmed that there is exist an optimal longitudinal pitch to diameter ratio S_L/d minimizing the tube absorber volume. It is about 1.0 to 1.1 depending on the tube diameter.

The present model was not considered to the effect of solution droplets. Actually, the pressure drop in the shell side of the horizontal tube absorber can be higher than higher than the results obtained from this study.

References

[1] G. Grossman, "Simultaneous heat and mass transfer in film absorption under laminar flow", International Journal of Heat and Mass Transfer, Vol. 26, No. 3, pp. 357-371, 1983.

[2] T. Nishimura, "Flow across tube banks", Encyclopedia of Fluid Mechanics, Vol. 1, pp. 763-785, 1986.

[3] F. Zdravistch, C. A. Fletcher, M. Behnia, "Numerical laminar and turbulent fluid flow and heat transfer predictions in tube banks", International Journal of Numerical Method for Heat and Fluid Flow, Vol. 5, pp. 717-733, 1995.

[4] Y. O. Wang, L. A. Penner, S. J. Ormiston, "Analysis of laminar forced convection of air or crossflow in banks of staggered tubes", Numerical Heat Transfer, Part A, Vol. 38, pp. 819-845, 2000.

[5] A. S. Wilson, M. K. Bassiouny, "Modeling of heat transfer for flow across tube banks", Chemical Engineering and Processing, Vol. 39, pp. 1-14, 2000.

[6] H. Suzuki, W. Nagamoto, T. Sugiyama, "Simulation on vapor flow in the absorber/evaporator of an absorption chiller", Transactions of the JSRAE, Vol. 20, No. 3, pp. 325-331, 2003.

[7] Y. A. Çengel, Heat Transfer, A Practical Approach, The McGraw-Hill Companies, Inc., 1998.

[8] S. V. Partankar, C. H. Liu, and E. M. Sparrow, "Fully develop flow and heat transfer in ducts having streamwise-periodic variations of cross-sectional area", Journal of Heat Transfer, Vol. 99, pp. 180-186, 1977.

[9] FLUENT 5 User's Guide, Fluent Incorporated, 1998.

[10] S. V. Partankar, "Numerical heat transfer and fluid flow", Hemisphere Publishing Co., Washington, D.C., 1980.

[11] T. Nishimura, Y. Kawamura, "Analysis of flow across tube banks in low Reynolds number region", Journal of Chemical Engineering of Japan, Vol. 14, pp. 267-272, 1981.

Author Profile

Thanh Tong PHAN

Birth: 1973, 1996: B.Eng., Hochiminh City Univ. of Technology (HUT), VIETNAM. 2000: Lecturer, HUT. 2002: M.Eng., Pukyong Natl Univ. (PKNU), KOREA. Current: Ph.D. Student, PKNU, Dept. of Refrigeration and Air- conditioning Engg.

Jung-In Yoon

Birth: 1961. 1988: B.Eng., Pukyong Natl Univ. (PKNU), KOREA. 1995: Ph.D.Eng., Tokyo Univ. of A&T, JAPAN. Current: Associate Prof., Pukyong National University, School of Mechanical Engg.

Eun-Pil Kim

Birth: 1962. 1987: B.Eng., Pusan Natl Univ., KOREA. 1991: M.Eng., Univ. of Pittsburgh, USA. 1995: Ph.D.Eng., Univ. of Pittsburgh, USA. Current: Associate Prof., Pukyong National Univ., KOREA, Shool of Mechanical Engg.